

## OH/F substitution in topaz studied by Raman spectroscopy

M. V. B. Pinheiro, C. Fantini, K. Krambrock, A. I. C. Persiano, M. S. S. Dantas, and M. A. Pimenta  
*Departamento de Física - ICEX, Universidade Federal de Minas Gerais, CP 702, 30123-970 Belo Horizonte, MG, Brazil*  
 (Received 5 September 2001; revised manuscript received 16 November 2001; published 20 February 2002)

The Raman band related to the stretching mode of hydroxyl ( $\text{OH}^-$ ) centered at about  $3650\text{ cm}^{-1}$  is investigated in several natural specimens of topaz single crystals with a composition  $\text{Al}_2\text{SiO}_4(\text{OH}_x\text{F}_{(1-x)})_2$  within a wide range of OH mole fractions ( $x$ ). The analysis of the OH band shape shows that its asymmetry is due to an unresolved splitting in two peaks, centered at  $3639$  and  $3647\text{ cm}^{-1}$ , labeled as  $\text{OH}_A$  and  $\text{OH}_B$ , respectively. Although the asymmetry is drastically different for OH-rich and OH-poor topaz, we show that this is only caused by the change of the  $\text{OH}_A/\text{OH}_B$  intensity ratio with the total OH concentration. In order to explain the splitting of the OH band, we suggest a model which involves a reduction of the local symmetry from  $D_{2h}^{16}$  to  $C_{2v}^9$ , resulting in two types of physically nonequivalent F sites (A and B) where the OH/F substitution can occur. Both sites have  $C_1$  site symmetries and a multiplicity of 4.

DOI: 10.1103/PhysRevB.65.104301

PACS number(s): 63.20.Pw, 61.66.Fn

## I. INTRODUCTION

For more than a half-century the vibrational spectra of topaz, a solid solution of chemical formula  $\text{Al}_2\text{SiO}_4(\text{OH}_x\text{F}_{(1-x)})_2$ , where  $0 < x < 0.3$ , have been a matter of intensive investigations using Raman<sup>1-5</sup> and infrared spectroscopies.<sup>5-13</sup> Most of these studies were related to the investigation of the symmetry of topaz as well as the OH/F substitution. Although no definitive answer has yet been established concerning the space group, much has been learned about the influence of the OH/F substitution on many of its physical properties such as, e.g., the refraction index and specific weight. On the other hand, much less is known about the relationship between the OH/F substitution and the concentration of color centers.

One of the first investigations of OH in topaz was done by Krishnan in 1947<sup>1</sup>. Besides the lattice modes and the fluorescence band attributed to  $\text{Cr}^{3+}$  impurity substituting for  $\text{Al}^{3+}$ , a Raman band related to the OH stretching mode at  $3649\text{ cm}^{-1}$  was also observed.<sup>1</sup> It was argued that the frequency of the OH infrared-absorption band at  $3600\text{ cm}^{-1}$  was fairly coincident with that of the frequency-shifted Raman band.<sup>1</sup> In the same work, Krishnan also reported the observation of a weak shoulder at about  $3636\text{ cm}^{-1}$ . No symmetry considerations involving group theory were done at that time.

In 1987, roughly 40 years after the work by Krishnan,<sup>1</sup> the Raman spectra of a fluorine-rich topaz single crystal was systematically investigated by Beny and Piriou.<sup>4</sup> Based on a complete group theory analysis for a topaz structure having a  $D_{2h}^{16}$  space group, the lattice modes were assigned to the Raman peaks and compared to the polarized infrared spectra. Hydroxyl modes were found at  $3650$  and  $1165\text{ cm}^{-1}$ .<sup>4</sup> The band at  $3650\text{ cm}^{-1}$  was, in the same way as mentioned in Ref. 1, also decomposed in two components at  $3639$  and  $3650\text{ cm}^{-1}$ .<sup>4</sup> These two peaks were assigned to two proper vibrations (stretching modes) of the OH molecule substituting for F.<sup>4</sup> In addition to these two lines around  $3650\text{ cm}^{-1}$ , the Raman band at  $1165\text{ cm}^{-1}$  was assigned to the in-plane bending mode of the OH molecule.<sup>4</sup> Later, in 1992, an infra-

red study of topaz confirmed the existence of a band related to the Al-OH bending mode at  $1150\text{ cm}^{-1}$ , as well as a band related to the stretching mode of OH at about  $3600\text{ cm}^{-1}$ .<sup>12</sup> Although the intensity of the  $3600\text{ cm}^{-1}$  band varied drastically from sample to sample, possibly due to the variable OH content, no splitting was found in the infrared spectrum.<sup>12</sup> The strong pleochroism of the infrared band was also intensively investigated,<sup>7,8,10</sup> and recently explained by the orientation of the OH dipoles in a direction tilted at  $27.3^\circ$  from the  $c$  axis in the (010)plane.<sup>13</sup>

With the advent of the topaz synthesis, and in particular of its OH end-member  $\text{Al}_2\text{SiO}_4(\text{OH})_2$ ,<sup>14,15</sup> the OH molecule was again investigated. Wunder *et al.*<sup>14</sup> observed a splitting of the  $3640\text{ cm}^{-1}$  single asymmetric OH IR band of a natural F-rich topaz in two components centered at  $3600$  and  $3520\text{ cm}^{-1}$  for their synthetic OH topaz. To explain such a splitting, it was suggested that either (i) a lowering of the overall symmetry from a  $D_{2h}^{16}$  ( $Pbnm$ ) group to a noncentrosymmetric group  $C_{2v}^9$  ( $Pbn2_1$ ) group, resulting in two distinct sites with different vibrational frequencies; or (ii) that the doubling of the OH vibrations arises from nondegenerate OH splitting, i.e., Davydov splitting,<sup>14</sup> which was also supposed in Ref. 4.

However, lowering of the overall symmetry from  $D_{2h}^{16}$  to  $C_{2v}^9$  is not yet well understood. Although several structural studies based on x-ray data confirm a  $D_{2h}^{16}$  space group for natural topaz (e.g., Ref. 16), local distortions, resulting in two types of nonequivalent lattice sites for F, with different nearest-neighbor distances, thus supporting a lower symmetry, were also reported.<sup>14-16</sup> For OH-rich natural samples, another possibility for a lowering of the  $D_{2h}^{16}$  symmetry, to an accentric triclinic  $C_1^1$  ( $P_1$ ) group, was also proposed.<sup>17,18</sup> An ordering of the OH is usually described as the cause of this symmetry lowering. Both  $C_{2v}^9$  and  $C_1^1$  symmetries would allow pyroelectricity and piezoelectricity to be observed, while the same would not occur for a  $D_{2h}^{16}$  symmetry. In fact, there is experimental evidence for pyroelectric and piezoelectric effects in topaz (as reported, e.g., in Ref. 19), but such effects are only anomalies which are consistent with a possible local

symmetry reduction to a non-centrosymmetric group as proposed in Ref. 17.

In this work we present a Raman investigation of the influence of the OH molecules substituting for F as a function of the total OH concentration over a broad range, i.e.,  $0 < x < 0.3$ . Special attention is given to the splitting of the Raman band, which is associated with the  $A_g$  stretching mode of the hydroxyl molecule near  $3650 \text{ cm}^{-1}$ . A model for the splitting that takes into account the lowering of the local symmetry is also proposed.

## II. SAMPLES AND EXPERIMENTAL SETUP

Twenty-seven natural gem-quality single crystals of topaz were investigated in this work. The samples were sorted in two distinct groups (see Table I): type-I samples, with high OH content; and type-II samples, with low OH content. Most type-I samples (TC1-TC11) were colored specimen (Imperial Topaz, from Ouro Preto, Minas Gerais, Brazil) ranging from yellow to pink. The type-I sample THK was a pink topaz from Katlang district (Pakistan). Type-II colorless samples came with two exceptions from Mexico (THD1-THD11, THT). The other two were from Brazil, TRO1 (Rondônia) and TMG1 (Minas Gerais), the former pale blue and the latter colorless.

The F content of all samples was determined using electron microprobe analysis in the wavelength dispersive mode of a Jeol JXA-8900RL spectrometer. The measurement parameters were a spot diameter of 20 nm, an acceleration voltage of 15 kV, and a sampling of about 5–10 points per sample with a counting time of 10 s. The compositions in percent of weight (wt %) of F were obtained with help of standards;  $\text{CaF}_2$  and  $\text{NdF}_3$ . The F-content results for samples THT (Zacatecas, Mexico) and THK (Katalang, Pakistan) were in good agreement with an earlier analysis (see Ref. 19, Table 3.1). In order to check the accuracy of the microprobe analysis, the F content was also indirectly estimated for several samples by means of the refraction indexes  $n_x$  and  $n_y$ , measured with a gemmological refractometer (Eickhorst) (see Refs. 19 and 20 for details of the calculation). The results, including the OH molar content ( $X_{OH}$  in percent), are listed in Table I.

For the Raman measurements a DILOR XY spectrometer has been used, with an argon-ion laser as an excitation source ( $\lambda = 514.5$  and  $457.9 \text{ nm}$ ). The typical spectral resolution was  $2 \text{ cm}^{-1}$ . All spectra were recorded at room temperature using a backscattering configuration, and with the light polarized along the  $c$  axis of the topaz samples, thus perpendicular to their basal cleavage plane (001).

## III. EXPERIMENTAL RESULTS

Four representative Raman spectra of the OH band related for type-I and -II samples with different OH contents are shown in Fig. 1, after normalization of the intensity using the  $\text{SiO}_4$  lattice mode Raman band at  $936 \text{ cm}^{-1}$ . For comparison, the  $\text{Cr}^{3+}$  background luminescence band of the colored topaz specimen was subtracted [Fig. 1(a)]. The spectra shown in Fig. 1 represent all types of topaz found in nature,

TABLE I. Investigated topaz single crystals with their color, F content as determined by electron microprobe analysis in wt %, OH molar fraction based on the microprobe analysis, and F content in wt % estimated from the refraction indexes  $n_x$  and  $n_y$ .

Sample	Color	wt % (F)	$X_{OH}$ (%)	wt % (F) ( $n_x, n_y$ )
Type I (OH-rich)				
TC1 <sup>a</sup>	Yellow	$16.0 \pm 0.2$	23	-
TC2 <sup>a</sup>	Yellow	$16.0 \pm 0.2$	23	$16 \pm 2$
TC3 <sup>a</sup>	Yellow	$14.7 \pm 0.1$	29	-
TC4 <sup>a</sup>	Yellow	$14.7 \pm 0.1$	29	$15 \pm 1$
TC5 <sup>a</sup>	Yellow	$15.7 \pm 0.1$	24	-
TC6 <sup>a</sup>	Orange	$16.1 \pm 0.3$	22	$16 \pm 1$
TC7 <sup>a</sup>	Orange	$15.7 \pm 0.1$	24	-
TC8 <sup>a</sup>	Orange	$16.3 \pm 0.3$	21	$15 \pm 2$
TC9 <sup>a</sup>	Pink	$15.5 \pm 0.3$	25	$16 \pm 1$
TC10 <sup>a</sup>	Pink	$15.0 \pm 0.4$	28	$15 \pm 1$
TC11 <sup>a</sup>	Pink	$15.4 \pm 0.1$	26	-
THK <sup>b</sup>	Pink	$15.2 \pm 0.2$	27	$15 \pm 1$
Type II (OH-poor)				
THD1 <sup>c</sup>	Colorless	$19.6 \pm 0.2$	5	$21 \pm 2$
THD2 <sup>c</sup>	Colorless	$20.7 \pm 0.2$	0	-
THD3 <sup>c</sup>	Colorless	$20.8 \pm 0.2$	0	$19 \pm 2$
THD4 <sup>c</sup>	Colorless	$19.7 \pm 0.2$	5	-
THD5 <sup>c</sup>	Colorless	$19.3 \pm 0.2$	7	$21 \pm 2$
THD6 <sup>c</sup>	Colorless	$20.7 \pm 0.2$	0	$21 \pm 2$
THD7 <sup>c</sup>	Colorless	$20.7 \pm 0.2$	0	$19 \pm 2$
THD8 <sup>c</sup>	Colorless	$20.7 \pm 0.2$	0	$21 \pm 2$
THD9 <sup>c</sup>	Colorless	$20.5 \pm 0.2$	1	$20 \pm 2$
THD10 <sup>c</sup>	Colorless	$20.0 \pm 0.2$	3	$21 \pm 2$
THD11 <sup>c</sup>	Colorless	$20.5 \pm 0.1$	1	$21 \pm 2$
THT <sup>d</sup>	Colorless	$20.7 \pm 0.2$	0	-
TRO1 <sup>e</sup>	Pale blue	$17.8 \pm 0.1$	14	$20 \pm 1$
TMG1 <sup>f</sup>	Colorless	$18.0 \pm 0.1$	13	-

<sup>a</sup>Ouro Preto (Brazil).

<sup>b</sup>Katlang (Pakistan). Fluorine content known from Ref. 16, Table 3.1:  $15.78 \text{ wt } \%$  (F).

<sup>c</sup>Durango (Mexico).

<sup>d</sup>Zacatecas, San Luiz Potosi (Mexico). Fluorine content known from Ref. 16, Table 3.1:  $20.2 \text{ wt } \%$  (F).

<sup>e</sup>Rondônia (Brazil).

<sup>f</sup>Marambaia (Brazil).

with extremes in the concentration of OH. The shapes of the bands are clearly different. The bands of all type-I samples and two of the type-II samples (TRO1 and TMG1) can be decomposed into two Gaussian lines centered at  $3639$  and  $3647 \text{ cm}^{-1}$ , which we call  $\text{OH}_A$  and  $\text{OH}_B$ , respectively. For OH contents lower than 10% ( $x < 0.1$ ), e.g., sample THD5, only one band was observed ( $\text{OH}_B$ ) at  $3647 \text{ cm}^{-1}$  [Fig. 1(c)]. For samples with  $x < 0.07$ , no band was detected in this spectral region [Fig. 1(d)].

Figure 2(a) shows the Raman spectrum of the OH-rich type I sample (TC1) as a function of the laser power ( $\lambda = 514.5 \text{ nm}$ ). Figure 2(b) shows the same spectrum for excitation light with two different wavelengths of the Ar laser:

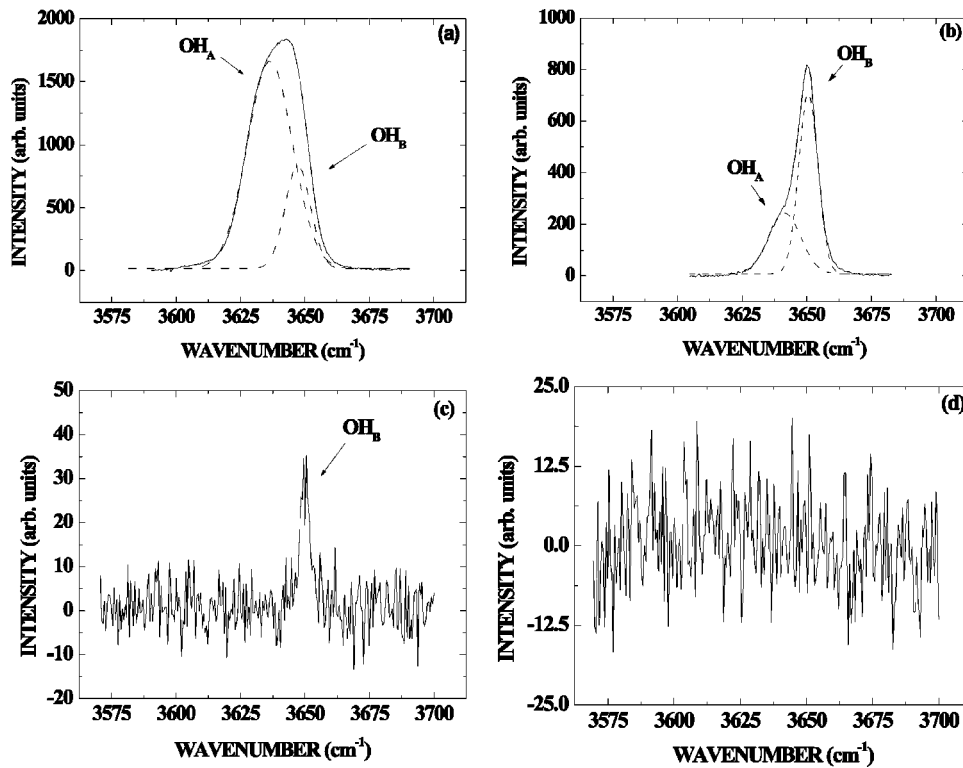


FIG. 1. Raman lines associated with the OH stretching mode, after normalization of the intensity with the  $\text{SiO}_4$  lattice mode measured at 300 K with the light polarized along the  $c$  axis and an excitation wavelength of 514.5 nm: (a) sample TC1, OH -rich ( $X_{\text{OH}} = 23\%$ ); (b) sample TMG1, intermediate OH ( $X_{\text{OH}} = 13\%$ ); (c) sample THD5, OH -poor ( $X_{\text{OH}} = 7\%$ ); (d) sample THD2 ( $X_{\text{OH}} < 5\%$ ).

514.5 nm (green) and 457.9 nm (blue). The spectra of Figs. 2(a) and 2(b) consist mainly of the asymmetric Raman band centered at about  $3650 \text{ cm}^{-1}$ .

From Fig. 2(a) one can see that the band positions and shapes are independent of the excitation, a result which is expected for Raman bands and not for features due to electronic transitions, e.g., luminescence. For excitation with the green line of the laser a superposition with the onset of a broad red luminescence band was observed, which is related to the crystal-field transitions of  $\text{Cr}^{3+}$  substituting for  $\text{Al}^{3+}$  in a distorted octahedral site.<sup>1</sup> The same does not occur for the blue excitation. Similar spectra were observed for all type-I samples (Imperial topaz), with drastic differences both on the intensity of the luminescence band and asymmetry of the OH band.

Since type-I samples absorb in the visible range, mostly in blue and violet spectral regions, one could argue that the linewidths in such samples could be broadened, when compared to the Raman bands of type-II samples (colorless), due to a local heating by the green excitation light (see Fig. 1). However, this idea is easily ruled out by the observation that increasing excitation power has no visible effect on the band shape [Fig. 2(b)]. The spectra of colorless OH-poor type-II topaz are much different from OH-rich type-I samples. While for a few THD samples, such as for example, THD5, it was possible to observe a very weak symmetric band near  $3649 \text{ cm}^{-1}$  [Fig. 1(c)] for the other samples this band was not measurable. On the other hand, the Raman spectra of samples TRO1 and TMG1 readily yielded an asymmetric band centered at  $3650 \text{ cm}^{-1}$ . Even though there are differences in the intensity, position, and band shape for type-I and -II samples, this band can be attributed to the stretching mode of the hydroxyl molecule (OH) which is incorporated

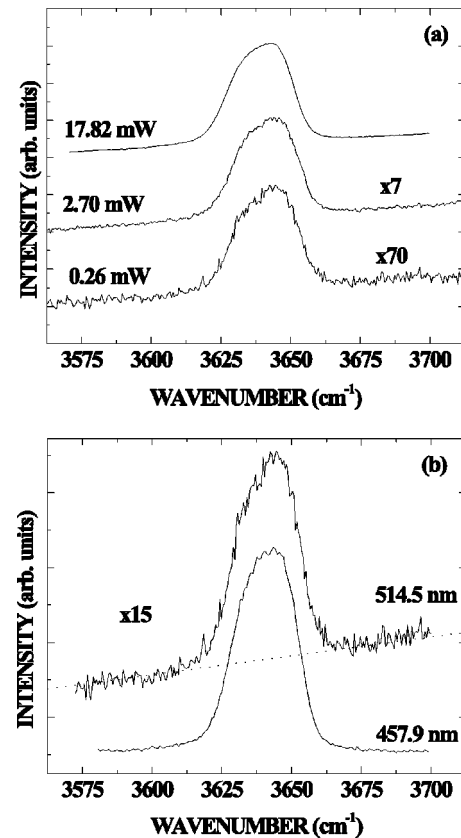


FIG. 2. Raman spectra of OH-rich topaz (TC1) (a) for three excitation powers using the green line of an Ar laser and (b) for two excitation wavelengths of the Ar laser. The inclined backgrounds are due to the superposition of the OH band with the  $\text{Cr}^{3+}$  red luminescence.

into the topaz lattice substituting for F.

Along with the drastic intensity difference, there are two main features that differ in the spectra of type-I and -II samples. The first is the strong luminescence band of  $\text{Cr}^{3+}$ , which was not observed in type-II samples, indicating that the concentration of trace  $\text{Cr}^{3+}$  in type-II samples is much lower than for type-I samples. This is expected since the color center responsible for the pink in the OH-rich type-I sample (Imperial topaz) is related to the  $\text{Cr}^{3+}$  substituting for  $\text{Al}^{3+}$ .<sup>19</sup> The second feature is the shape of the OH band, which is clearly different from that of the type-I spectra.

#### IV. DISCUSSION

The Raman spectra for two samples, one OH-poor (TRO1) topaz and one OH-rich (TC6) topaz, were measured for the following symmetries  $Z(YY)Z$ ,  $Z(XX)Z$ ,  $X(ZZ)X$ ,  $X(ZY)X$ , and  $Y(ZX)Y$ ,  $Z(YX)Z$ . For the first three, no difference in the line shape was observed, and for the last three no band could be detected. Therefore, it was not possible to apply the method described in Ref. 24 for inferring the direction of the OH vibration. For the investigation of the site occupation as a function of the total OH content, for convenience we chose a backscattering configuration with the light polarized along the  $c$  axis of the topaz samples, thus perpendicular to their basal cleavage plane (001).

Earlier results of a Raman study of a single topaz crystal, carried out at 77 K,<sup>25</sup> revealed an OH-band with a lineshape very similar to what we observed at room temperature for samples with low OH concentrations. For both, no splitting could be resolved without fitting the line shape with two Gaussian peaks. Therefore, the asymmetric OH Raman band was fitted with two Gaussian peaks as a function of the total OH content. The fit parameters are shown in Figs. 3(a), 3(b), and 4 as function of the OH mole fraction. We observe in Fig. 3(a) that the peak positions shift to lower frequencies as the OH content increases. This is expected since the  $c$  parameter is insensitive to the OH/F substitution, whereas the  $a$  and  $b$  lattice parameters increase, thus increasing the volume of the unit cell.<sup>19</sup> Figure 3(b) shows that the peak widths increase with the OH concentration, indicating that the lattice disorder also increases with  $x$ . Therefore, a possible ordering of the lattice with the OH/F substitution resulting in a  $C_1^1$  symmetry, can be ruled out. The disorder, that increases the width of the peaks and decreases the Raman shifts as  $x$  becomes higher, may also be related to impurities which are incorporated in the lattice like, e.g.,  $\text{Cr}^{3+}$  and  $\text{Fe}^{3+}$  substituting for  $\text{Al}^{3+}$ . These impurities were observed by electron paramagnetic resonance and x-ray fluorescence in higher concentrations for the OH-rich samples than for the OH-poor samples,<sup>21</sup> as expected for larger unit cell and lattice sites.

The natural questions that arise after this analysis are the following: (i) Why do the intensities of the  $\text{OH}_A$  and  $\text{OH}_B$  Raman peaks change with total OH content? (ii) Can each band be associated with a specific type of site? To answer the first question we must analyze Fig. 4. It shows the relative normalized integrated intensities for the two OH lines as a function of  $x$ . It can be observed that the intensity of the  $\text{OH}_B$  peak saturates at a lower level than that of the  $\text{OH}_A$  peak.

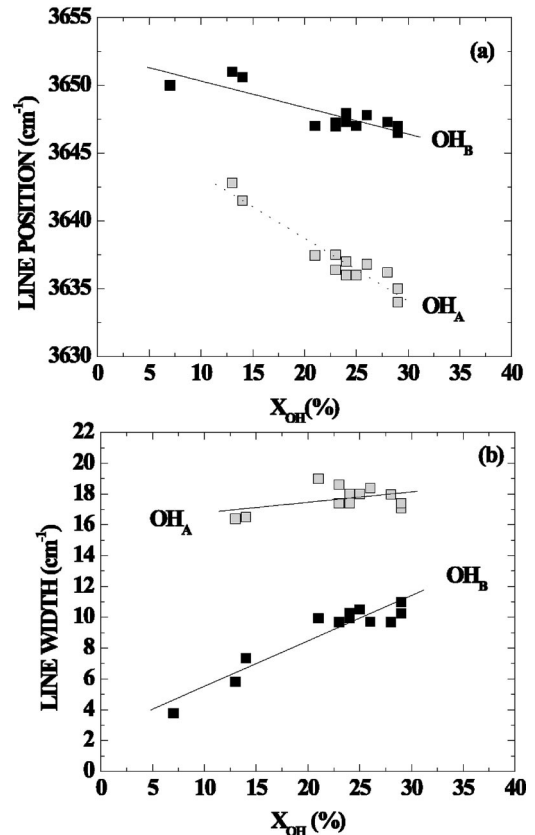


FIG. 3. Dependence of band positions (a) and bandwidths (b) of the  $\text{OH}_A$  and  $\text{OH}_B$  Raman lines as a function of OH content. The lines are from the best linear fit and serve as guide to the eyes.

The  $\text{OH}_B$  peak, that dominates the spectrum at lower OH contents, is rapidly surpassed by the  $\text{OH}_A$  peak as  $x$  increases. This result indicates that the substitution of F by OH at B sites is more favorable for lower  $x$ , whereas, for higher  $x$ , as the volume of the unit cell increases, the situation is reverted and the A sites become more occupied.

This is true if we consider that there are two different types of sites in the topaz lattice where the substitution F/OH

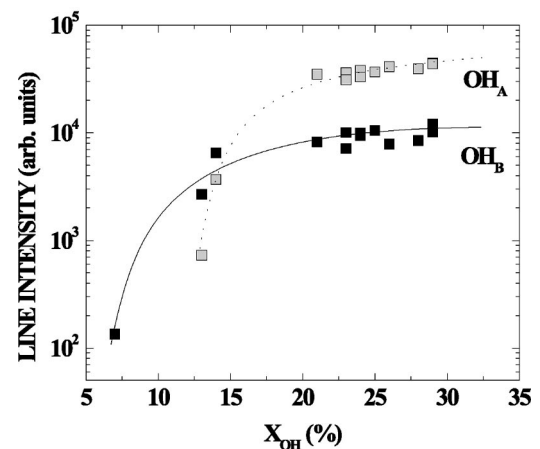


FIG. 4. Dependence of the integrated intensity of the peaks  $\text{OH}_A$  and  $\text{OH}_B$  as a function of the fluorine content. The curves are guide to the eyes.

TABLE II. Al - (F,OH) bond lengths in Å, after structural refinements, for the two types of nonequivalent sites *A* and *B* related to the two Raman peaks  $\text{OH}_A$  and  $\text{OH}_B$ .

Site	$x = 1$ <sup>a</sup>	$x = 0.28$ <sup>a</sup>	F topaz <sup>b</sup>	OH-Topaz <sup>b</sup>	$X$ unknown <sup>c</sup>
<i>A</i>	1.833(2)	1.802(1)	1.788(1)	1.826(1)	1.791(2)
<i>B</i>	1.834(2)	1.808(1)	1.798(1)	1.834(1)	1.801(2)
<i>B-A</i>	0.001(2)	0.006(1)	0.010(1)	0.008(1)	0.010(2)

<sup>a</sup>Reference 14.

<sup>b</sup>Reference 15.

<sup>c</sup>Reference 16.

can take place. This leads us to the second question. In fact, precise structural refinements of synthetic OH-topaz,  $\text{Al}_2\text{SiO}_4(\text{OH})_2$ , as well as on natural topaz, confirmed that the two types of F sites indeed have bond lengths different from the neighbor Al. This is shown in Table II. Since both F sites have different lengths for their bonds with the nearest neighbors their sites are physically distinct.

In order to relate the  $\text{OH}_A$  and  $\text{OH}_B$  peaks (site *A* and *B*) with the two different F sites where the OH/F substitution takes place, the integrated intensity of the OH peak as a function of  $x$  has to be considered. From Figs. 1 and 4, it is clear that the site related to the  $\text{OH}_B$  peak becomes occupied first, i.e., for lower  $x$ . It is expected that the site with larger volume and thus larger bond length to first neighbors becomes occupied first. Therefore, we ascribe the two OH peaks,  $\text{OH}_A$  and  $\text{OH}_B$ , to F/OH sites with smaller and larger Al-F/OH bond lengths, respectively, as shown in Table II and Fig. 5.

For a  $D_{2h}^{16}$  space group of a topaz structure with four molecules per unit cell, one would expect eight possible equivalent F/OH sites with a  $C_1$  point symmetry.<sup>22</sup> Even though refinements of x-ray data reveal differences in the bonds of F sites due to local distortions,<sup>14–16</sup> the space group usually assumed for the interpretation of x-ray-diffraction data is the  $D_{2h}^{16}$  which has exactly the same systematic extinctions as the  $C_{2v}^9$  group.<sup>14</sup> For a  $D_{2h}^{16}$  space group one would expect a single OH Raman band due to the eight equivalent  $C_1$  sites available for the OH/F substitution.<sup>19</sup>

On the other hand, our experimental results show that two types of nonequivalent sites for the F/OH substitution may

exist in the unit cell. Therefore, we must have four equivalent positions for each type of site, which is incompatible with a  $D_{2h}^{16}$  symmetry. In this case each type of site will have a  $C_1$  point symmetry if the space group is  $C_{2v}^9$ , and the number of Raman peaks will be two instead of one expected for  $D_{2h}^{16}$  symmetry. This is consistent with our observation of two OH Raman peaks, as well as earlier attempts to explain the doubling of the OH infrared line in synthetic topaz.<sup>14</sup> A symmetry reduction to a  $C_1$  group is readily discarded, since for this case all F sites where the substitution may occur are nonequivalent  $C_1$  sites, thus yielding eight Raman peaks instead of two. The critical point for this model is how to conciliate a possible local  $C_{2v}^9$  symmetry resulting in two physically distinct types of sites for F in the unit cell, with the well accepted  $D_{2h}^{16}$  symmetry as determined from x-ray data where F occupies only one type of site  $C_1$ . If the two types of sites are non-equivalent and the short-range symmetry is  $C_{2v}^9$ , as observed by Raman, there may be a twinning-like static disorder or a dynamical disorder<sup>23</sup> at long range capable of averaging the two types of nonequivalent sites in a macroscopic  $D_{2h}^{16}$  average symmetry as observed by x-ray diffraction. This type of disorder is consistent with evidence of textural sectors with anomalous optical, piezoelectrical, and pyroelectrical properties of topaz,<sup>17</sup> also corroborating evidence from neutron-diffraction studies which suggests a lower symmetry for topaz.<sup>18</sup> In order to confirm a local  $C_{2v}^9$  symmetry, and to investigate either the short- and long-range symmetry-dependent texture of topaz and its relationship with disorder, symmetry-sensitive experiments are still detrimental. It should be noted that colored specimens of natural topaz are always related to higher substitutions of F by OH, possibly favored by the disorder and the greater unit cell.

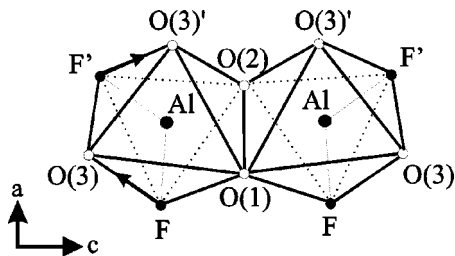


FIG. 5. Local environment around two  $\text{Al}^{3+}$  ions of the topaz structure with a  $C_{2v}^9$  symmetry showing the two nonequivalent F sites (F and  $F'$ ) located at the unshared octahedral edges. These two sites correspond to the two frequencies of  $\text{OH}_A$  at F and  $\text{OH}_B$  at  $F'$ . The approximate directions of the OH vibrations, as determined in Ref. 13, are also shown in the figure. These directions are about  $27.3^\circ$  from the  $c$  axis in the (010) plane (the plane of the figure).

## V. SUMMARY

The Raman spectra of natural topaz samples were reported and analyzed for a broad range of OH concentrations including OH-rich (colored) and OH-poor (colorless) samples. The asymmetry of the Raman band at about  $3650\text{ cm}^{-1}$ , attributed to the OH stretching mode, is explained as an unresolved splitting from two distinct OH-related peaks centered at about  $3639\text{ cm}^{-1}$  ( $\text{OH}_A$ ) and  $3647\text{ cm}^{-1}$  ( $\text{OH}_B$ ). From the behavior of the frequency shifts and widths of the two Raman peaks, we conclude that their dependence with

OH content is caused by disorder, possibly induced by the OH/F substitution and the higher concentration of impurities in the OH-rich topaz. The changes in the relative intensities of the two peaks with the OH content is related with an unequal substitution of F by OH in two physically distinct sites in the unit cell, the *A* and *B* sites, thus causing two distinct proper frequencies. Finally, we conclude that in order to explain the splitting of the Raman band associated with the stretching mode of the OH molecule in topaz, a lowering of the local symmetry from the  $D_{2h}^{16}$  group to the  $C_{2v}^9$  group is required.

## ACKNOWLEDGMENTS

This work was supported by the Brazilian agencies FAPEMIG, CAPES (Grant Nos. BEX0356/00 and Probral 125/01), and CNPQ/RHAE. We are indebted to Professor Joachim Karfunkel (IGC/UFMG) for many motivating discussions, as well as to Dr. Don Hoover for providing us several samples used in this work. We are also grateful to Dr. Fernando S. Lameiras (CDTN) and Digeórgia N. da Silva for the use of the refractometer of the Gemlab and to William T. Soares for the help with the microprobe analysis.

- 
- <sup>1</sup>R. S. Krishnan, Proc.-Indian Acad. Sci., Sect. A **26**, 460 (1948).  
<sup>2</sup>W. P. Griffith, J. Chem. Soc. A **9**, 1372 (1969).  
<sup>3</sup>J. E. Griffiths and K. Nassau, Appl. Spectrosc. **34**, 395 (1980).  
<sup>4</sup>J. M. Beny and B. Piriou, Phys. Chem. Miner. **15**, 148 (1987).  
<sup>5</sup>B. S. Wang and J. Tu, Spectrosc. Spectral Anal. **20**, 41 (2000).  
<sup>6</sup>D. M. Adams and D. J. Hills, J. Chem. Soc. Dalton Trans. **16**, 1562 (1977).  
<sup>7</sup>W. Gebert and J. Zeeman, Neues Jahrb. Mineral. Monatsh **1965**, 380.  
<sup>8</sup>G. Isseti and A. M. Penco, Period. Mineral. Rome **36**, 380 (1967).  
<sup>9</sup>R. Brunel and R. Vierne, Bull. Soc. Fr. Mineral. Cristallogr. **93**, 328 (1970).  
<sup>10</sup>F. Gervais, B. Piriou, and J. L. Servoin, Bull. Soc. Fr. Mineral. Cristallogr. **96**, 81 (1973).  
<sup>11</sup>L. T. Kovaleva, Zh. Prikl. Spektrosk. **22**, 311 (1975).  
<sup>12</sup>C. A. Londos, A. Vassilikou-Dova, G. Georgiou, and L. Fytros, Phys. Status Solidi A **133**, 473 (1992).  
<sup>13</sup>K. Shinoda and N. Aikawa, Phys. Chem. Miner. **21**, 24 (1994).  
<sup>14</sup>B. Wunder, D. C. Rubie, C. R. RossII, O. Medenbach, F. Seifert, and W. Schreyer, Am. Mineral. **78**, 285 (1993).  
<sup>15</sup>P. A. Northrup, K. Leinenweber, and J. B. Parise, Am. Mineral. **79**, 401 (1994).  
<sup>16</sup>Yu. V. Ivanov, E. L. Belokoneva, J. Protas, N. K. Hansen, and V. G. Tsirelson, Acta Crystallogr. Sect. B: **54**, 774 (1998).  
<sup>17</sup>M. Akizuki, M. S. Hampar, and J. Zussman, Miner. Mag. **43**, 237 (1979).  
<sup>18</sup>J. B. Parise, C. Cuff, and F. H. Moore, Miner. Mag. **44**, 943 (1980).  
<sup>19</sup>D. B. Hoover, *Topaz* (Butterworths-Heinenmann, Oxford, 1992), p. 40.  
<sup>20</sup>P. H. Ribbe and P. E. Rosenberg, Am. Mineral. **56**, 1812 (1971).  
<sup>21</sup>M. V. B. Pinheiro and K. Krambrock (private communication).  
<sup>22</sup>D. L. Rousseau, R. P. Bauman, and S. P. S. Porto, J. Raman Spectrosc. **10**, 253 (1981).  
<sup>23</sup>A. Jório, M. S. S. Dantas, C. B. Pinheiro, N. L. Speziali, and M. A. Pimenta, Phys. Rev. B **57**, 203 (1998).  
<sup>24</sup>S. Klauer and M. Woehlecke, Phys. Rev. Lett. **68**, 3212 (1992).  
<sup>25</sup>J. T. Koproge and R. L. Frost, Spectrochim. Acta, Part A **56**, 501 (2000).